STUDIES ON NANO-INDENTATION OF POLYMERIC THIN FILMS USING FINITE ELEMENT METHODS

Shen Xiaojun, Yi Sung, Lallit Anand
Singapore-MIT Alliance
E4-04-10, 4 Engineering Drive 3, Singapore 117576
Zeng Kaiyang
Institute of Materials Research and Engineering
3 Research Link, Singapore 117602

Abstract—In this paper, the numerical simulation for nano-indentation is performed to measure time-dependent behavior of polymeric films. The possibility to extract the relaxed shear modulus of the polymer is evaluated using a rigid ball indenter. The viscoelastic behavior of the polymer was represented by the standard model. The effects of Poisson's ratio are also discussed.

1. Introduction

Thin polymer films have been widely used in electronic industries. Thermo-mechanical properties and residual stresses generated in polymeric films on silicon substrates are of special interests in microelectronic packaging. During the curing and post-curing processes, polymer films form three-dimensional crosslinkings and shrinks, which results in developing a large amount of stresses in silicon substrates and polymeric films. In addition, the adhesion strength of polymer films to substrates is crucial to their successful performance.

Nano-indentation is now widely used to measure the mechanical properties, such as modulus, hardness and adhesion, with the emphasis on thin films due to its nanometer displacement resolution. The most extensively used method to extract Young's modulus and Poisson's ratio by nano-indentation is proposed by W. C. Oliver and G. M. Pharr [1], in which load-displacement curve during unloading is used to calculate the equivalent Young's modulus. The materials response is assumed to be elastoplastic during loading and fully elastic in unloading [1].

Although its success in extracting mechanical properties for metal and ceramic thin films, challenges have been encountered when trying to use Oliver and Pharr's method to extrapolate useful information from nanoindentation data on polymers due to the time dependent nature of the polymer samples [2]. In most cases, the elastic modulus calculated from various polymers based upon nanoindentation data are elevated 20 – 30% relative to the values obtained with more standard tests. This larger E is believed to be due to tip-sample adhesion, that effectively increases the contact area of the tip during indentation, and creep which increases the slope of unloading curve. The rate sensitive nature of polymers also causes 'nose phenomenon' in indentation [3]. Many efforts have been done to eliminate creep effect to get more accurate Young's modulus [4]-[9]. However, it seems that the time dependent nature of Young's modulus is neglected and the polymers response is assumed to be elastoplastic. To extract time dependent properties of polymers by nano-indentation is a tackle task. Some researchers used standard solid model to represent the viscoelastic properties, and obtained the coefficients before the differential operators by curve fitting of the ball

indentation creep test [10-13]. This demonstrates that, nano-indentation is a potential technique to measure the viscoelastic properties of polymeric thin films.

2. Basic Theory

In practice, sharp indentation tests are frequently used to extract the Young's modulus and hardness from the unloading curve of an indentation experiments. Owing to the large rotations induced by the sharp indenter, a large strain formulation of the problem is warranted.

For ball indentation, however, axisymmetry prevails and linear kinematics is sufficient at moderate indentations. For classical elasto-plastic materials, the well-known experimental findings by Tabor have been given a solid theoretical background by Hill *et al.* [14] and Biwa and Storakers [15]. When time dependence is modeled by linear visco-elasticity, pertinent to many polymers at small strains, the theoretic frame of ball indentation is already known.

Perhaps the first ones to presents a solution to the problem of ball indentation of incompressible linear viscoelastic materials were Lee and Radok [17]. Their approach was to tentatively replace the materials constants in the classical elastic solution with the corresponding differential operators in the viscoelastic constitutive equation. Hunter extended the solution to linear viscoelastic materials when Poisson's ratio is constant [18]. A more general solution to the problem was presented by Graham [19].

The mechanical behavior of the materials of interest is assumed to be isotropic and linearly viscoelastic. Using ordinary notation the stress-strain relation can then be formulated in relaxation form as

$$s_{ij} = \int_0^t G_1(t-\tau)\frac{d}{d\tau} e_{ij}\, d\tau \qquad (1)$$

$$\sigma_{kk}(t) = \int_0^t G_2(t-\tau)\frac{d}{d\tau}\sigma_{kk}(\tau)d\tau \qquad (2)$$

where

$$S_{ij} = \sigma_{ij} - \frac{1}{3}\delta_{ij}\sigma_{kk},$$

$$e_{ij} = \varepsilon_{ij} - \frac{1}{3}\delta_{ij}\varepsilon_{kk} \qquad (3)$$

It has been tacitly assumed above that $\sigma_{ij}=\varepsilon_{ij}=0$ for $t<0$.

Furthermore, within linear kinematics the relation between strains and displacements is

$$\varepsilon_{ij} = \frac{1}{2}(u_{i,j} + u_{j,i}) \qquad (4)$$

while quasi-static equilibrium with body forces absent becomes

$$\sigma_{ij,i} = 0 \qquad (5)$$

It is assumed that a perfectly spherical and rigid ball is pressed onto a viscoelastic half-space under axisymmetric conditions. If the ball diameter D is sufficiently larger than the contact radius a, the displacement boundary condition is

$$u_3 = h - r^2/D, x_3 = 0, r \le a$$

It is also assumed that no friction between ball and half-space, the boundary condition within the contact area are

$$\sigma_{31} = \sigma_{32} = \sigma_{33} = 0, x_3 = 0, r > a \qquad (6)$$

The general solution is

$$h = \frac{1}{R^{1/3}}\left[\frac{3\pi}{4}K * dP\right]^{2/3} \qquad (7)$$

where K*dP stands for the function defined by the Riemann-Stieltjes integral, and

$$K(t) = \left[\frac{1}{\pi}(2G_1 + G_2) * d\Lambda^{-1} * dG_1^{-1}\right](t) \qquad (8)$$

$$\Lambda(t) = G_1(t) + 2G_2(t) \qquad (9)$$

If the viscoelastic material of the half space has similar behavior in shear and dilatation then, the Poisson's ratio is

constant. K is given through the equation

$$K(t) = \frac{1-\nu}{\pi} G_1^{-1}(t) \qquad (10)$$

Because the history effect of viscoelastic materials, the analysis of the usual indentation loading and unloading cycle is difficult. It is suitable to use indentation creep test, in which the force is applied in a time as short as possible and is held for a period time, at same time the depth is recorded.

In an indentation creep test, the force can be represented by

$$P = P_0 h(t) \qquad (11)$$

where h(t) is Heaviside unit step function. Under the condition of constant Poisson's ratio, equation (7) becomes

$$G_1(t) = \frac{3}{4}(1-\nu) P_0 \frac{1}{h^{3/2} R^{1/2}} \qquad (12)$$

Therefore from indentation creep tests, shear modulus of the material of half-space can be extract if its Poisson's ratio is known.

In general, Poisson's ratio is changing with time. However, at reasonable experiment time, the amplitude of Poisson's ratio's changes is small. In this study, it assumed that it is constant, and the shear modulus can be estimated through equation (12).

3. Results of FEM Simulation

Because the stress and strain fields under the indentation tip are complicated, finite element method is a very useful tool to study indentation problem. In this study, ABAQUS 5.8 is employed. The mesh used in all the simulations is depicted in Fig 1. In view that no Saint-Venant principle is available for the contact problem, the outer boundaries were taken at least about 50 times the maximum contact length away from the indented area. The indentation creep is achieved by moving the rigid ball to a prescribed depth, then adding the equivalent force and maintain it, at the same time lift the boundary restriction for the rigid ball. And no friction between the rigid ball and the surface of the samples.

1. Simulation results of indentation on standard solid

The material analyzed was assumed to have the standard solid behavior. The radius of the rigid ball is taken as 2 μm. The instantaneous value of Young's modulus is 3 GPa. The Poisson's ratio is 0.3 and keeps constant. The retardation time τ is assumed to be 2 s. The relaxed shear modulus can be represented by Prony's expression:

$$G_R(t) = G_0\left(1 - g_a(1 - e^{-t/\tau})\right) \qquad (13)$$

where g_a is assumed to be 0.4.

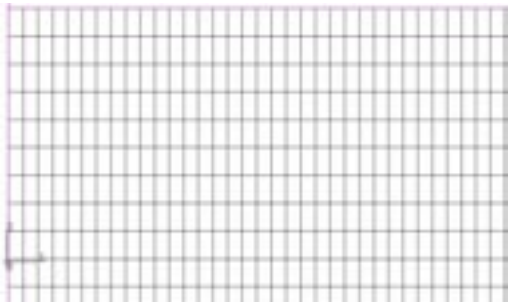

Fig. 1, Mesh used in simulation

The bulk modulus has the same time expression as equation (13).

In the simulation, the creep time is taken as 30 seconds.

Fig. 2 illustrates the creep depth, it increases very fast within 2 seconds, then the increasing becomes slow, and the curve becomes flat at about 15 seconds. The total depth increasing is over 40%.

Fig. 3 shows the strain field at the moment of just loading the force and the moment of 30 seconds of force holding. It can be seen that, the strain is nearly 10 percent just under the tip, therefore careful attention should be paid when the indentation method is

used to extract the linear viscoelastic properties.

Fig. 4 shows the shear modulus obtained from equation (12), together with the theoretic shear modulus. It can be seen that the difference between the inputted relaxed shear modulus and the shear modulus calculated is less than 10 percent. Thus, it would be safe to extract the shear modulus using equation (12) at a certain range.

2. Effects of Poisson's ratio on the creep depth

The changing of Poisson's ratio makes indentation problems more complicated to handle with. The results of two situations are presented in Fig. 5. One situation is Poisson's ratio is constant with the value of 0.3, the other is the results of bulk modulus is constant with the initial Poisson's ratio value of 0.3.

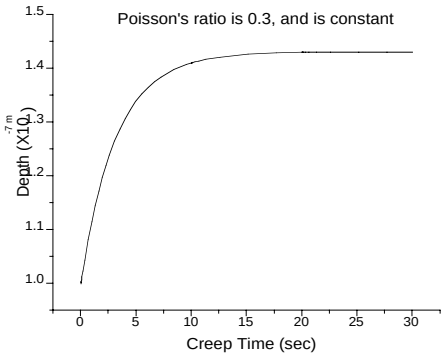

Fig. 2, The creep depth

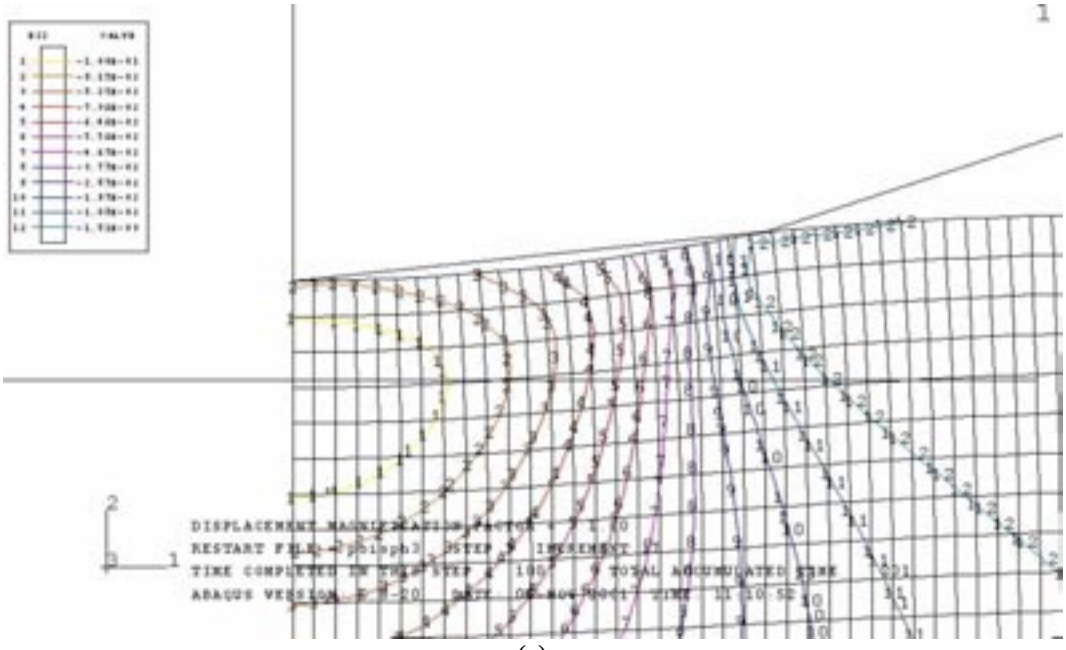

(a)

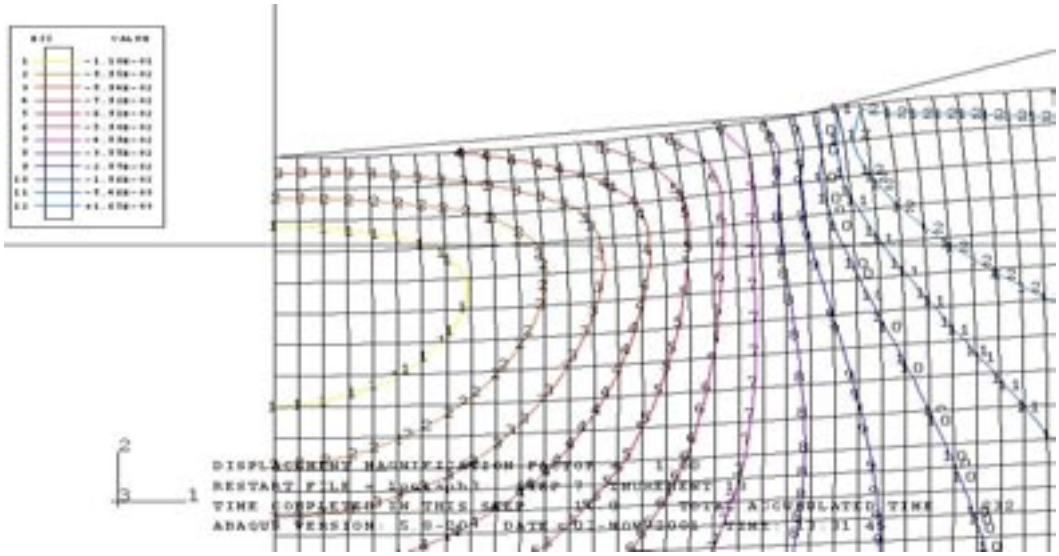

(b)

Fig. 3, Strain field. (a) just after force is loaded; (b) after 30 s of force holding

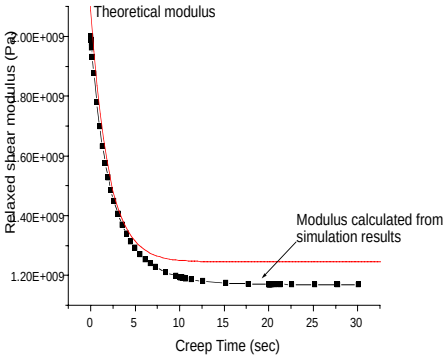

Fig. 4, Relaxed shear Modulus

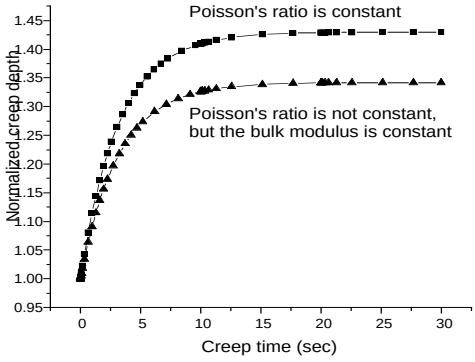

Fig. 5. The difference between the normalized creep depths of constant Poisson's ratio and the constant bulk modulus

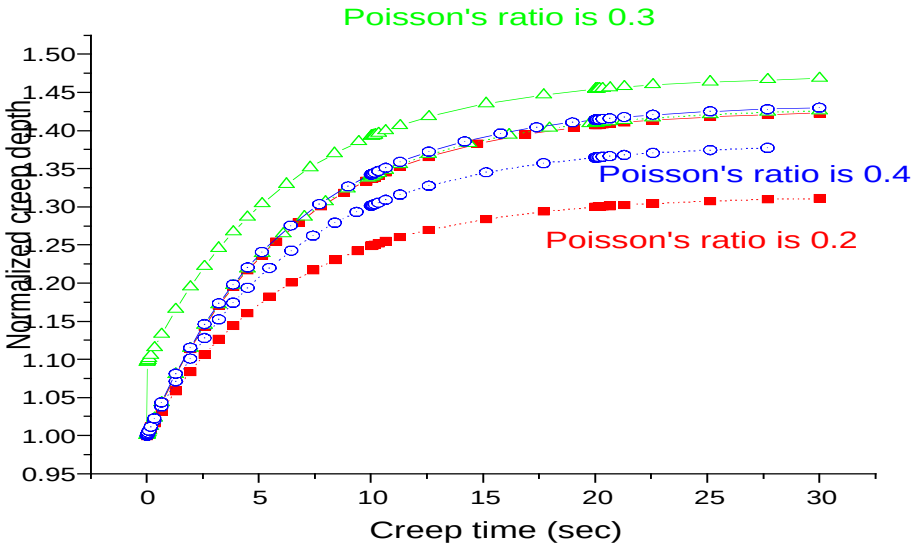

Fig. 6. The normalized creep depth for different initial Poisson's ratio. Solid line for constant Poisson's ratio, dash line for constant bulk modulus. The retardation time is 4 seconds.

_the initial Poisson's ratio is 0.2
❒the initial Poisson's ratio is 0.3
⓪the initial Poisson's ratio is 0.4

From Fig. 5, it can be seen that, within the retardation time, the creep depths are nearly the same. After the retardation time, the difference increases with time and becomes constant at 10 seconds. The maximum difference is less than 10 percent.

Fig. 6 illustrates the differences between the normalized depths for various Poisson's ratios. As shown in Fig. 6, the maximum difference for the same initial Poisson's ratio is about 10 percent. The differences decrease with increasing the initial value of Poisson's ratio. By considering the error of nano-indentation is 10 percent, it could be reasonable to use equation (12) to estimate the relaxed shear modulus.

3. The effect of retardation time

The results of normalized depth for retardation of 2 seconds and 4 seconds with the constant Poisson's value of 0.3 are illustrated in Fig. 7. It shows that, when the retardation time is small, the depth increases faster. However, when time reaches 30 seconds, the normalized depth is nearly the same since the infinite shear moduli are identical for the two situations. We might estimate the instantaneous and infinite modulus through the depth reached just after the loading of the force and the depth at the time when the depth curve is flat.

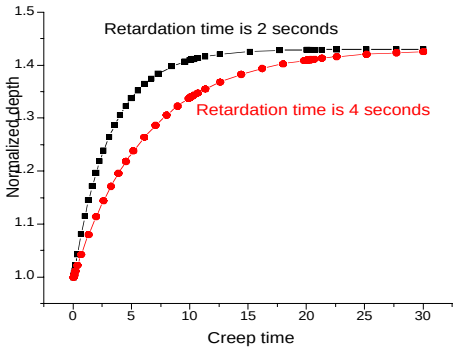

Fig. 7. The effect of retardation time. The Poisson's ratios for the two curves are all 0.3.

4. Conclusion

Rigid ball indentation creep test can be used to measure or estimate the relaxed shear modulus as an alternative to traditional testing method, when the indentation depth is shallow.

Reference

1. W. C. Oliver and G. M. Pharr. An improved technique for determining hardness and elastic modulus using load and displacement sensing indentation experiments, J. Mater. Res. **7**, 1564 (1992)
2. B. J. Briscoe, L. Fiori and E. Pelillo. Nano-indentation of polymeric surfaces, J. Phys. D: Appl. Phys., 70, 2395 (1998)
3. B. J. Briscoe and K. Savio Sebastian. The elastoplastic response of poly(methyl methacrylate) to indentation, Proc. R. Soc. Lond. A **452**, 439 (1996)
4. Strojny, X. Y. Xia, A. Tsou and W. W. Gerberich. Techniques and considerations for nanoindentation measurements of polymer thin film constitutive properties, J. Adhesion Sci. Technol. **2**, 1299 (1998)
5. P. Grau, H. Meinhard and S. Mosch. Nanoindentation experiments on glass and polymers at different loading rates and the power law analysis, Mat. Res. Soc. Symp. Proc. **522**, 153 (1998)
6. Min Li, C. Barry Carter and W. W. Gerberich. Nano-indentation measurements of mechanical properties of polystyrene thin films, Mat. Res. Soc. Symp. **649**, (2001)
7. N. S. Lawson, R. H. Ion, H. M. Pollock, D. J. Hourston and M. Reading.

Characterising polymers surfaces – nanoindentation surface force data, calorimetric microscopy, Physica Scripta. **T55**, 199 (1994)
8. M. J. Adams, D. M. Gorman and S. A. Johnson. Nanoindentation of poly (methyl methacrylate), Mat. Res. Soc. Symp. Proc. **649**, (2001)
9. M. Oyen-Tiesma, Y. A. Toivola and R. R. Cook. Load-displacement behavior during sharp indentation of viscous-elastic-plastic materials, Mat. Res. Soc. Symp. **649**, (2001)
10. X. Xia, A. Strojny, L. E. Scriven, W. W. Gerberich. Constitutive property evaluation of polymeric coatings using nanomechannical methods, Mat. Res. Soc. Symp. Proc. **522**, 199 (1998)
11. L. S. Cheng, L. E. Scirven and W. W. Gerberich. Viscoelatic analysis of micro- and nanoindentation, Mat. Res. Soc. Symp. Proc. **522**, 193 (1998)
12. A. Strojny, W. W. Gerberich. Experimental analysis of viscoelastic behavior in nanoindentation, Mat. Res. Soc. Symp. Proc. **522**, 159 (1998)
13. K. B. Yoder, S. Ahuja, K. T. Dihn, D. A. Crowsong, S. G. Coreoran, L. Cheng and W. W. Gerberich. Nanoindentation of viscoelastic materials: mechanical properties of polymer coatings on aluminum substrates, Mat. Res. Soc. Symp. Proc. **522**, 205 (1998)
14. D. Tabor, The Hardness of Metals, 1951, Clarendon Press, Oxford.
15. Hill, R., Storakers, B. and Zdunek, A., A Theoretical Study of the Brinell Hardness Test. Proc. Royal Soc. Lond., , **A423**, 301 (1989)
16. Biwa, S. and Storakers, B., An Analysis of Fully Plastic Brinell Indentation. J. Mech. Phys. Solids, **43**, 1303 (1995)
17. E. H. Lee and J. R. M. Radok. The contact problem for viscoelastic bodies, J. Appl. Mech. **27**, 438 (1960)
18. S. C. Hunter. The Hertz problem for a rigid spherical indenter and a viscoelastic half-space, J. Mech. Phys. Solids **8**, 219 (1960)
19. G. A. C. Graham. The contact problem in the linear theory of viscoelasticity, Int. J. Engng Sci. **3**, 27 (1965)